Biomech Model Mechanobiol (2011) 10:651–661
DOI 10.1007/s10237-010-0263-1

ORIGINAL PAPER

A novel experimental procedure based on pure shear testing of dermatome-cut samples applied to porcine skin

Marc Hollenstein · Alexander E. Ehret · Mikhail Itskov · Edoardo Mazza

Received: 31 May 2010 / Accepted: 15 October 2010 / Published online: 11 November 2010

Abstract This paper communicates a novel and robust method for the mechanical testing of thin layers of soft biological tissues with particular application to porcine skin. The key features include the use of a surgical dermatome and the highly defined deformation kinematics achieved by pure shear testing. Thin specimens of accurate thickness were prepared using a dermatome and were subjected to different quasi-static and dynamic loading protocols. Although simple in its experimental realisation, pure shear testing provides a number of advantages over other classic uni- and biaxial testing procedures. The preparation of thin specimens of porcine dermis, the mechanical tests as well as first representative results are described and discussed in detail. The results indicate a pronounced anisotropy between the directions along and across the cleavage lines and a strain rate-dependent response.

Keywords Pure shear · Soft tissue testing · Dermatome · Skin · Dermis · Anisotropy · Preconditioning

M. Hollenstein (✉) · E. Mazza
Institute for Mechanical Systems, ETH Zurich,
8092 Zurich, Switzerland
e-mail: mhollenstein@ethz.ch

A. E. Ehret · M. Itskov
Department of Continuum Mechanics, RWTH Aachen University,
Aachen, Germany
e-mail: ehret@km.rwth-aachen.de

M. Itskov
e-mail: itskov@km.rwth-aachen.de

E. Mazza
EMPA, 8600 Duebendorf, Switzerland
e-mail: emazza@ethz.ch

1 Introduction

Mechanical characterisation of biological tissues plays an essential role for the understanding of their behaviour and functioning. Likewise, testing represents the initial step for the development of constitutive models for these tissues, which in turn form the basis for computer simulations in many fields of research and engineering.

Ideally, biological materials are characterised in their physiological environment, which provides the biological and mechanical interactions with the surrounding tissues and fluids. However, the possibilities for in vivo testing are limited by technical feasibility on the one hand and by ethical aspects on the other hand. Typical soft tissue testing methods for in vivo application include indentation, pulling, suction or compression tests, e.g. on skin (Dobrev 1999; Delalleau et al. 2006) and porcine liver (Ottensmeyer 2002), intraoperative indentation and aspiration experiments on human liver (Carter et al. 2001; Nava et al. 2008), surface torsion (Kalanovic et al. 2003; Valtorta and Mazza 2006), pinching (Brouwer et al. 2001) and elastography methods (Sandrin et al. 2003; Rouvière et al. 2006; Klatt et al. 2007). Although similar to physiological loading conditions, the kinematic states achieved in these tests are generally not well-defined and highly inhomogeneous. Accordingly, when these experiments are used to determine the parameters of constitutive models, sophisticated and computationally intensive inverse optimisation routines with numerous degrees of freedom are necessary and the results are often unsatisfactory.

In vitro tests provide the possibility to create experimental data for kinematically rather simple load cases such as uni- or biaxial tension, compression or simple shear. Typically, the respective mechanical boundary value problems can be solved analytically and thus, based on these data, constitutive models can be calibrated in a straightforward manner. In vitro

characterisation of biological tissues is based on methods and protocols which are well-proven for testing of engineering materials. However, while the latter allow for tailoring of specimens of any shape and size, the sample geometry for biological tissues is restricted to its naturally grown dimensions and consequently often of a more primitive form.

A critical issue related to in vitro characterisation is the artificial behaviour induced by sample preparation and mounting. Waldman and Lee (2005) recently studied the effect of sample geometry on results in biaxial tension experiments with cruciform specimens. In their study, the arm length of the specimens had significant influence on the apparent extensibility of the material as well as on shearing and rotation of the sample. Butler et al. (1984) and Zernicke et al. (1984) discussed possible reasons for the large discrepancies and variations in the reported behaviour of tendons and fascia in uniaxial tension. Apart from many other factors, they identified the strain measurement technique to have a major effect. According to their results, at a certain maximum stress, the strains measured based on grip-to-grip distance were approximately three times larger than those measured optically in the central region of the specimen. These differences may be explained by tissue inhomogeneities on the one hand and clamping effects such as slippage or local tissue damage on the other hand. Clearly, also separation of the specimens from the tissue itself is prone to induce artefacts. In fact, by excision, physiological interactions are broken, the tissue structure is locally changed (see also Butler et al. 1984), artificial boundaries are created and physiological residual stresses are released. Finally, storage time and conditions between sample preparation and testing may have significant effect on the tissue properties.

Uniaxial loading represents the simplest test method from a technical point of view and has been used extensively for a long time to characterise soft biological tissues of various kinds. The load is usually applied such that the extension occurs under a uniaxial stress state with free lateral contraction. Tensile specimens are realised in different aspect ratios either as segments of the natural structure, e.g. tendons and muscle fascicles, or as strips cut from planar or bulky organs such as skin and arterial walls (e.g. Holzapfel et al. 2005). Compressive properties are studied in either constrained (e.g. Korhonen et al. 2002) or unconstrained (e.g. Van Loocke et al. 2008) compression tests. A general problem with compression tests is friction between sample and supports, which complicates the interpretation of the results (cf. Miller 2005). Planar tissues are frequently tested in biaxial tests implemented either as biaxial loading of cruciform (Waldman and Lee 2005) or rectangular specimens (Lanir and Fung 1974; Sacks 2000), or in inflation tests (Wineman et al. 1979). A major problem concerns the fixation of the planar specimens as discussed later in this paper. Finally, simple shear provides a method to characterise soft tissues and has for example been used to investigate myocardium (Dokos et al. 2002) and ligaments (Bonifasi-Lista et al. 2005).

Facing the importance of experimental data under different loading conditions for the formulation of constitutive models, it is surprising that the classic pure shear test, one of the simplest available tests, is rarely used in biomechanics. This test is usually realised by extending a thin rectangular specimen with a high width-to-length ratio on a uniaxial testing device. In fact, to the best of our knowledge, there are only two systematic applications of this test to soft tissues. Chu et al. (1972) performed in vivo and in vitro measurements in pure shear on cat mesentery in order to analyse the effects of perfusion, blood pressure, respiratory movements, and excision of the samples from the underlying organ on the obtained results. Recently, Gao et al. (2009) studied the behaviour of bulky isotropic liver parenchyma and emphasised the simplicity and reliability of the pure shear test. We remark that the deformation kinematics of pure shear has been realised in more complicated testing set-ups, where the lateral sample edges were fixed by sutures (Lanir and Fung 1974) or a biaxial testing device has been used (Sacks 2000) to restrict the lateral contraction.

In our work, we apply pure shear to anisotropic planar tissue samples of accurately defined thickness. Porcine dermis was chosen as a representative planar connective tissue with properties that are characteristic of the majority of soft collagenous tissues. These are strong non-linearity, very slight compressibility, viscoelasticity, softening and pronounced anisotropy. The preferred directions of the anisotropy coincide approximately with the optically observable cleavage lines of the skin (Cox 1942), which in turn result from the underlying diamond shape arrangement of collagen fibre bundles (Ridge and Wright 1966). Since there is a substantial amount of histological and biochemical similarities between porcine and human skin, the pig represents a useful animal model for skin research such as wound-healing studies (cf. Vardaxis et al. 1997).

2 Materials and methods

2.1 Sample preparation

The porcine dermis has a thickness of about 1–2 mm and is located just underneath the 30–140 μm thick epidermis (cf. Vardaxis et al. 1997). Dermal tissue is mainly composed of a dense three-dimensional network of collagen fibres and fibre bundles crossing each other in two main directions (Meyer et al. 1982). Depending on the anatomical site, also a substantial amount of elastic fibres are present (Meyer et al. 1981). Specifically, collagen and elastin are reported to constitute about 70–80% and about 4% of the dry weight, respectively (Mathews 1975; Fung 1993). Beneath the dermis, there

follows the subcutaneous layer, which primarily consists of fatty tissue and can take a thickness of over 12 mm depending on sex, anatomical site and nutritional state of the pig (cf. Vardaxis et al. 1997).

Skin pieces from the snout and head region of female domestic pigs (*sus scrofa domestica*) were obtained from the slaughterhouse immediately after animal slaughter. The pieces were approximately 300×300 mm large with a thickness of about 10–15 mm, leaving the tissue down to the subcutaneous layer intact. The skin pieces were transported in a cold box and then stored at 4°C in a refrigerator wrapped in physiological saline-soaked cloths. The samples were tested within 60 h of animal death. We remark that this time span may influence the tissue properties and should be reduced in a comparative study.

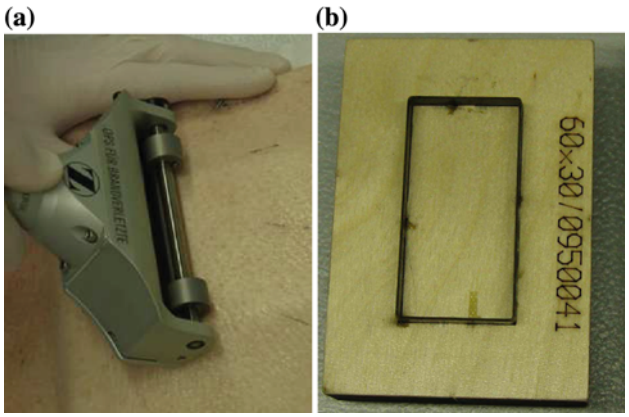

Fig. 1 **a** Separation of 500 μm thick dermis sections from skin pieces by means of a surgical dermatome. **b** Cutting die for the pure shear specimens

2.1.1 Preparation of the skin pieces

Skin pieces with a relatively uniform thickness were selected, carefully rinsed with water until clean and then dried with tissue paper. Subsequently, the pieces were shaved, first with an electrical hair trimmer to remove larger bristles and finally with a regular razor. After shaving, the cleavage lines (Langer 1861) became clearly visible and allowed for the estimation of the local preferred directions of fibre orientation. Pieces not directly further processed with the dermatome were again stored in saline-soaked cloths at 4°C.

2.1.2 Sample extraction by means of a dermatome

We used a wooden board with a rectangular foam damping pad of 80×120 mm attached to it as a mounting rack for dermatome cutting. The foam pad provided a compliant base for the skin pieces during cutting, similar to the soft fat and muscle tissue compound supporting the skin in situ. The cleaned and shaved skin pieces were mounted under slight tension over the damping pad and nailed on the circumference to the wooden board.

For sectioning the skin into precisely defined layers, we used an air-driven dermatome with a 80 mm width plate installed (Fig. 1a). The dermatome-cut thickness was set to 500 μm. According to standard surgical procedures, paraffine oil was applied to the skin in order to reduce friction between skin surface, dermatome and blade. The first layer contained the epidermis and was disposed. Sections two and three consisted completely of dermal tissue and were used for testing. We note that the first layer contracted considerably after excision revealing the presence of residual strains in situ. The effect was much less pronounced for the subsequent dermal layers.

Rectangular specimens were punched out of the dermis sections by the use of a die cutter with dimensions 30×60 mm (Fig. 1b). For punching, the dermis sections were carefully spread on saline-wetted tissue paper on an acrylic plate. The die was aligned with its long side either along or perpendicular to the optically observable cleavage lines in order to obtain *transversal* and *longitudinal* specimens. Pressing the punching tool onto the plate, the specimens were excised including the tissue paper as support.

For recovery from the preparation process, the ready-made samples were stored, wrapped in saline-soaked towels at 4°C for at least 2 h. 15 min before testing, the samples were taken to room temperature.

2.2 Experimental set-up

We performed the pure shear tests on a custom-made testing device. Two hydraulic actuators, each with 2.7 kN capacity and an available piston rod stroke of 100 mm, were mounted opposing, horizontally on a massive steel plate. A hydraulic power unit provided the two actuators with oil at 200 bar continuous pressure. Load cells with a capacity of 100 N were installed at the end of each actuator piston rod. Custom-made tissue clamps were directly attached to the load cells. The clamps made of titanium offered a clamping surface of 60×10 mm equipped with sandpaper of grade P320 to improve the grip. For contactless measurement of the in-plane strain field in the central region of the sample, a video extensometer system for triggered image acquisition was installed. The extensometer CCD camera equipped with a telecentric lens was mounted on a custom-made positioning frame for easy and accurate alignment. With a field of view of 32×32 mm, a resolution of 30 μm per pixel was obtained. A 4” white light LED-ring for optimal illumination of the measuring field was mounted at the end of the telecentric lens. The images were stored as 8-bit greyscale pictures. To isolate the test rig from ambient vibrations, the

Table 1 Technical specifications as for the dermatome and the experimental set-up including the video extensometer system

Unit/software	Type	Manufacturer	Specifications
Dermatome	Air dermatome	Zimmer	
Hydraulic actuators	242 Actuator	MTS Systems	2.7 kN capacity, 100 mm stroke
Hydraulic power unit	505 SilentFlo		200 bar pressure, 40 l/min capacity
External controller	793 FlexTest GT		
Control software	793 with MPT		
Load cells	SMT S-Type	Interface	100 N capacity
Video extensometer system	uniDAC FAST	Chemnitzer Werkstoffmechanik	
Image acquisition software	VEDDAC cam 3.2		
Image correlation software	VEDDAC 4.0		Digital image correlation, sub-pixel algorithm
CCD camera	Pike F-100B	Allied Vision Technologies	2/3" monochrome CCD, 1,000×1,000 pixels, 60 Hz frame rate, 8 bit greyscale pictures
Telecentric lens	NT55-349	Edmund Optics	32×32 mm field of view
Vibration control table	RS 2000, I-2000	Newport	

Manufacturer details: Zimmer Inc., Warsaw, IN, USA; MTS Systems Corp., Eden Praire, MN, USA; Interface Inc., Scottsdale, AZ, USA; Chemnitzer Werkstoffmechanik GmbH, Chemnitz, Germany; Allied Vision Technologies GmbH, Stadtroda, Germany; Edmund Optics GmbH, Karlsruhe, Germany; Newport Corp., Irvine, CA, USA

actuator positioning plate was fixed on a vibration control table. The technical details are summarised in Table 1.

2.3 Test realisation

The load cells were reset just before clamping of the tissue samples. A small supporting table was installed in between the clamps once the actuator piston rods were brought to their initial testing position (Fig. 2a), leaving a free gauge length of 10 mm. This table allowed precise and gentle spreading of the specimens on the support and the lower grip faces and carfully removing the tissue paper support with forceps.

After manually closing the clamps with a knurled thumb screw, the table could be carefully removed. Before running the test, physiological saline was sprayed onto the sample. In order to keep the sample moist at all times, the saline spray was reapplied at constant intervals.

For testing, one actuator piston rod was kept fixed at its initial testing position (passive actuator), while the opposing rod was driven under displacement control (active actuator).

After installation of the specimen and the removal of the clamping support (Fig. 2b), the sample was hanging slightly slack in-between the two clamps. To straighten the sample, the active actuator was retracted at 0.05 mm/s until a preload of 0.05 N was reached. This state demonstrated to be well reproducible, and we defined it as the reference state. Nominal strains and stresses were computed with respect to this state. The time between beginning of sample installation and test onset did not exceed 5 min.

The force acting on the passive actuator and the displacement of the active actuator relative to its initial position were

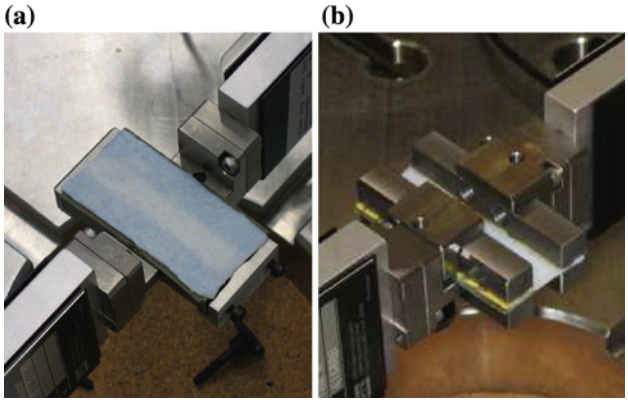

Fig. 2 Pure shear specimen after installation on the supporting table and lower grip faces **(a)**, and after closing the clamps and removal of the support **(b)**

sampled at 102.4 Hz, while the video extensometer recorded the deforming sample at 4 Hz.

The induced nominal (grip-to-grip) strain $\varepsilon_n(t)$, the stretch ratio $\lambda_n(t)$ and the engineering stress P were computed as

$$\varepsilon_n(t) = \frac{d(t)}{l_0}, \quad \lambda_n(t) = 1 + \varepsilon_n(t), \quad P = \frac{F(t)}{A_0}, \tag{1}$$

where the initial cross-sectional area A_0 (0.5×60 mm^2) was given, and the clamp displacement of the active actuator $d(t)$, the free gauge length at preload l_0 and the tensile force on the passive actuator $F(t)$ were measured.

2.4 Pure shear test protocol

We performed the tests in displacement-controlled mode, where the protocol was defined based on nominal strain and

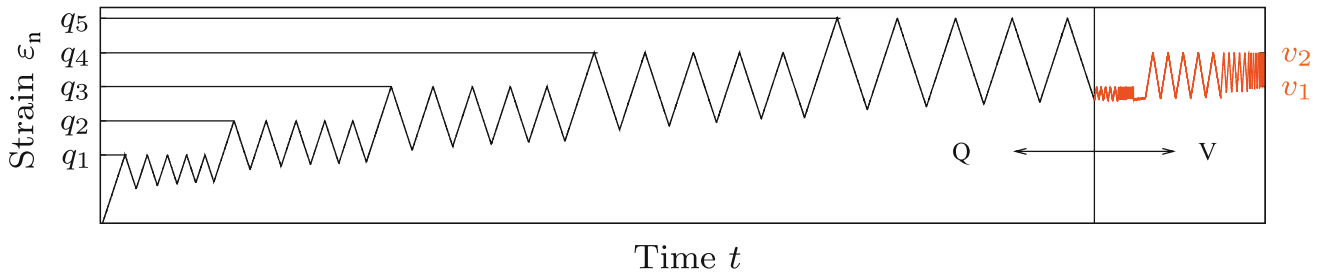

Fig. 3 Test protocol for the quasi-static preconditioning (Q) and cyclic loading (V). Nominal strain control is plotted over test time. While the upper load reversal points were predefined, the lower reversal points were enforced when the measured force became smaller than 0.05 N in order to prevent the tissue from becoming slack

Table 2 Strain level and strain rate specifications for the test protocol (Fig. 3)

q_1 [-]	q_2 [-]	q_3 [-]	q_4 [-]	q_5 [-]	v_1 [-]	v_2 [-]
0.057	0.086	0.114	0.143	0.171	q_3	q_4
r_0 [1/s]	r_1 [1/s]	r_2 [1/s]	r_3 [1/s]	r_4 [1/s]	r_5 [1/s]	
0.001	0.002	0.005	0.01	0.02	0.05	

strain rate. The lower cycle reversal points were enforced when the measured force became smaller than 0.05 N in order to prevent the tissue from becoming slack during the cyclic loading.

The protocol consisted of a quasi-static preconditioning of 5 cycles at strain rate r_0 on the strain levels q_1 to q_5 (Q) and 5 ramp cycles at increasing strain rates r_1 to r_5 on the strain levels v_1 and v_2, respectively (V, Fig. 3 and Table 2).

The highest strain level q_5 was chosen clearly below the rupture strain in preceding tension to failure experiments, and q_1 to q_4 were obtained by appropriate scaling. In order to determine the strain rate r_0 for quasi-static testing, we ran successive load cycles with gradually decreasing velocity. Below a certain limit, a further decrease in the strain rate had negligible effect on the force response. A strain rate of $r_0 = 0.001\text{s}^{-1}$ was identified to be sufficiently small.

2.5 Deformation kinematics

We consider the uniform extension of a body along three orthogonal axes specified by the orthonormal vectors $\boldsymbol{e}_i$, $i = 1, 2, 3$. In this case, the deformation gradient takes the form

$$\mathbf{F} = \sum_{i=1}^{3} \lambda_i \boldsymbol{e}_i \otimes \boldsymbol{e}_i, \tag{2}$$

where λ_i are the principal stretches. Assuming that the deformation is isochoric, they are related by the incompressibility constraint

$$J = \det \mathbf{F} = \lambda_1 \lambda_2 \lambda_3 = 1. \tag{3}$$

In the experiments, a thin specimen in the plane spanned by $\boldsymbol{e}_1$ and $\boldsymbol{e}_2$ is stretched by λ in the direction of $\boldsymbol{e}_1$. Considering samples with a high aspect ratio, i.e. the ratio between free length and width, uniform extension with free lateral contraction is obtained. Assuming incompressible behaviour (3), the principal stretches are given by $\lambda_1{=}\lambda$, λ_2 and $\lambda_3{=}1/(\lambda_1\lambda_2)$. On the other hand, with a decreasing aspect ratio, lateral contraction in the $\boldsymbol{e}_2$-direction becomes increasingly restricted, so that in the limit $\lambda_2{=}1$. This state is referred to as pure shear or strip biaxial extension. The respective stretches are given by $\lambda_1{=}\lambda$, $\lambda_2{=}1$, $\lambda_3{=}1/\lambda$.

In the present study, pure shear specimens with an aspect ratio of 1:6 were employed, which is smaller than the one recently applied by Gao et al. (2009), who worked with an aspect ratio of 1:4.

2.6 In-plane strain evaluation

A commercial image correlation software was used to trace a set of user-defined measuring points over the video extensometer images and determine their displacements. Based on this discrete displacement field, the in-plane strains were approximated by use of the finite element method.

The in-plane position $\boldsymbol{x}(\boldsymbol{X}, t)$ of a material particle of the specimen in the current configuration at time t is given by

$$\boldsymbol{x}(\boldsymbol{X}, t) = \boldsymbol{X} + \boldsymbol{u}(\boldsymbol{X}, t), \tag{4}$$

where $\boldsymbol{X}$ is the in-plane position of the particle in the reference configuration, and $\boldsymbol{u}(\boldsymbol{X}, t)$ is the corresponding in-plane displacement. The in-plane part $\mathbf{F}_{2\text{D}}$ of the deformation gradient (2) is thus obtained by

$$\mathbf{F}_{2\text{D}}(\boldsymbol{X}, t) = \frac{\partial \boldsymbol{x}(\boldsymbol{X}, t)}{\partial \boldsymbol{X}} = \mathbf{I}_{2\text{D}} + \frac{\partial \boldsymbol{u}(\boldsymbol{X}, t)}{\partial \boldsymbol{X}}, \tag{5}$$

where $\mathbf{I}_{2\text{D}}$ is the second-order identity tensor in two dimensions. The finite element interpolation of the displacement field based on a linear quadrilateral element yields

$$\boldsymbol{u}(\boldsymbol{X}) = \sum_{a=1}^{4} N^{(a)} \boldsymbol{u}^{(a)}, \tag{6}$$

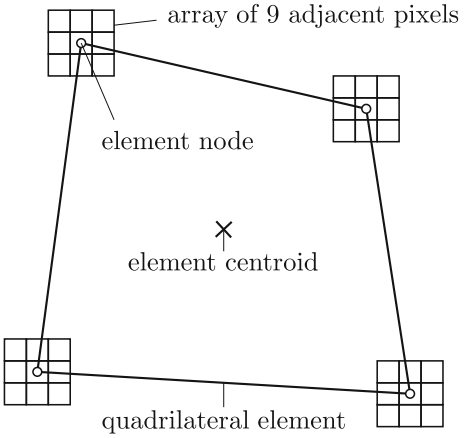

Fig. 4 Sketch of the *quadrilateral* element used to calculate in-plane strains. The nodal positions and displacements were obtained by averaging over nine adjacent measuring points (*pixels*)

with $\boldsymbol{u}^{(\mathrm{a})}$ being the in-plane displacements of the element nodes with respect to an image coordinate system and $N^{(a)}$ representing the shape functions. The deformation gradient (5) is thus approximated by

$$\mathbf{F}_{2\mathrm{D}}(\boldsymbol{X}) = \mathbf{I}_{2\mathrm{D}} + \sum_{a=1}^{4} \boldsymbol{u}^{(a)} \otimes \frac{\partial N^{(a)}}{\partial \boldsymbol{X}}. \tag{7}$$

The explicit dependence on time t has been omitted for the sake of brevity.

In this work, we used one single element adequately spanned over the free area of the specimens. To reduce the influence of stochastic errors, the positions and displacements of the four element nodes were obtained by averaging over nine adjacent pixels arranged in a 3×3 pattern, respectively (Fig. 4).

3 Results

A representative set of data is presented for a longitudinal and a transversal sample, which were both obtained from the same skin piece. The time span between these two tests was less than 1.5 h.

3.1 Quasi-static preconditioning

A distinct anisotropic response of the tissue was observed (Fig. 5). The tissue was considerably stiffer along the cleavage lines than perpendicular to them. The specimens showed substantial preconditioning effects such as softening, residual deformations and a tendency to stabilise after some cycles. Even for loading at low strain rates, the stabilised loading–unloading cycles demonstrate substantial hysteresis, a phenomenon usually referred to as pseudo-elasticity in biomechanics (Fung 1993). All response curves are characterised by the J-shape typical for the majority of soft biological tissues with a clearly distinguished linear region at higher stretch ratios.

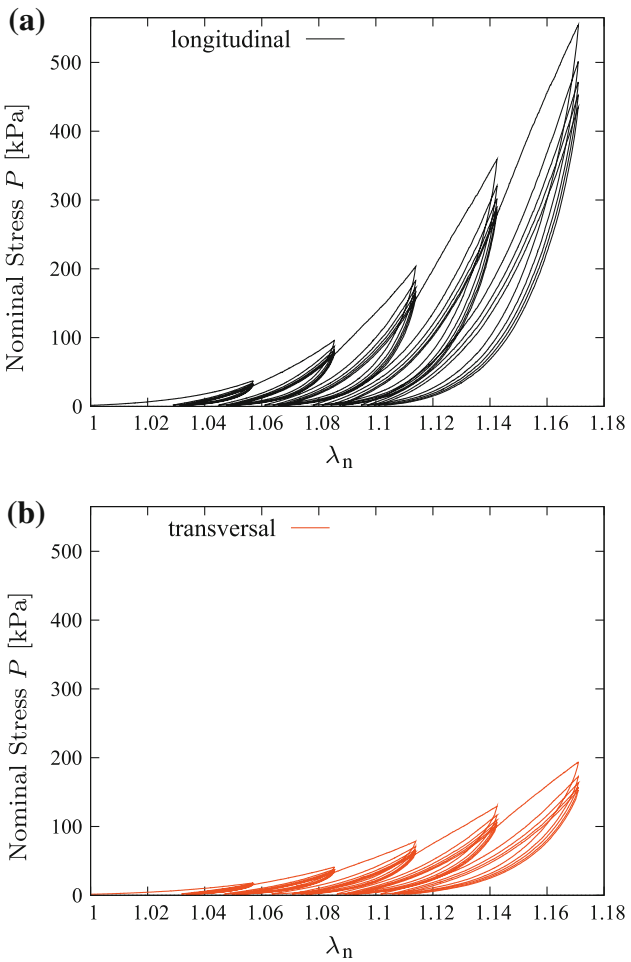

Fig. 5 Nominal stress response of a longitudinal **(a)** and transversal **(b)** porcine dermis sample to the quasi-static preconditioning protocol Q in a pure shear experiment

3.2 Viscoelastic behaviour

The response of the dermal specimens generally depended on the strain rate (Fig. 6). It was observed that during cyclic loading, the response tends to become stiffer with increasing strain rate (Fig. 6 top). Similar behaviour was observed for the peak stresses reached at the peak strains v_1 and v_2 after stabilisation. For further investigation of this issue, we considered the ratio between these peak stresses P_i and P_1 in the respective last cycle for each strain rate r_i, $i = 1, 2, 3, 4$. Plotting this ratio against the strain rate suggests that the influence of the strain rate on the peak stress decreases with the strain level (Fig. 7). The first five cycles at v_1 and v_2 with a strain rate of 0.002 s^{-1} deserve closer attention. While at the level

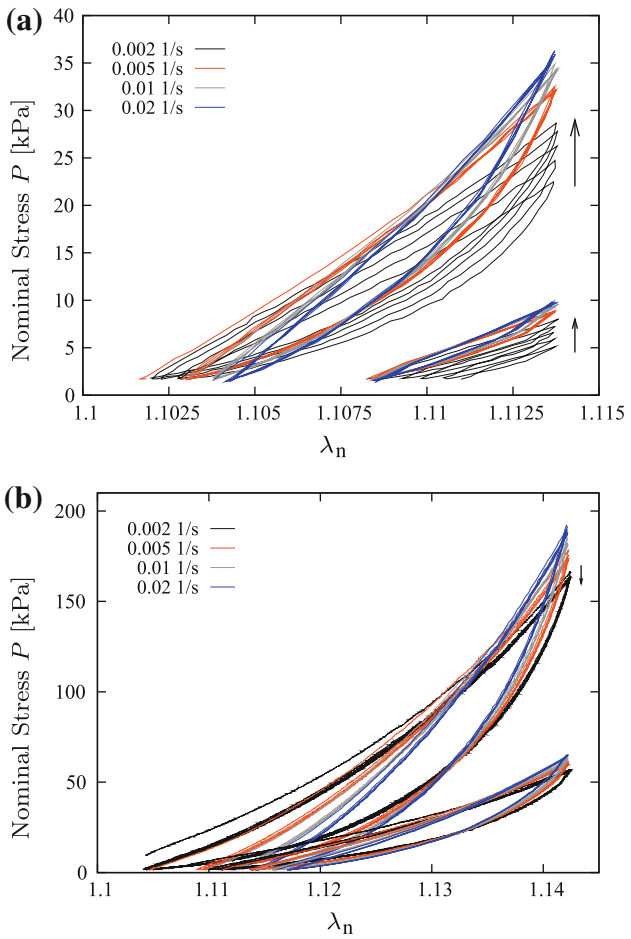

Fig. 6 Nominal stress response of a longitudinal and transversal porcine dermis sample to the protocol V at strain levels v_1 **(a)** and v_2 **(b)**. The *black arrows* indicates the direction of stabilisation during the five cycles at a strain rate of 0.002 s^{-1}

v_1 the curves stabilise towards a stiffer behaviour, only slight stabilisation to a softer behaviour occurs at the higher strain level v_2. If noticeable, the stabilisation direction is indicated by arrows in Fig. 6.

We remark that the data for the strain rate r_5 were not considered in the results due to a too small number of data points per cycle.

3.3 Comparison of nominal and in-plane strains

Nominal (ε_n) and optically measured in-plane strains (ε_p^a) were compared based on the difference $\rho_a = \varepsilon_p^a - \varepsilon_n$. Likewise, the deviation ρ_l of the optically determined lateral strain ε_p^l from the ideal case of zero contraction was considered, so that $\rho_l = \varepsilon_p^l$. Thereby, the in-plane strains were determined from the deformation gradient (7) evaluated at the element centroid according to Sect. 2.6.

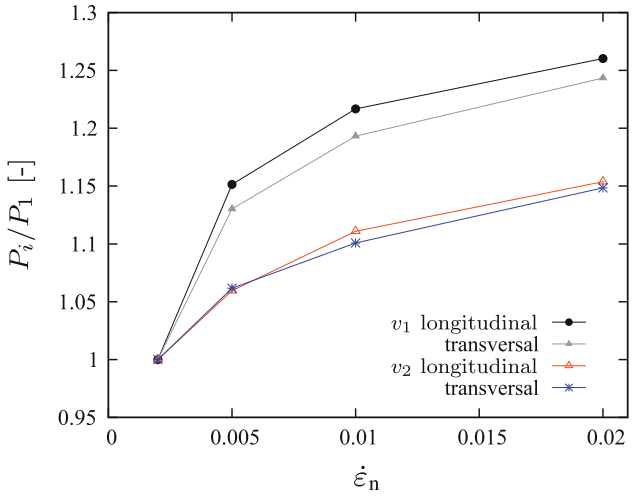

Fig. 7 Dependence of the peak stress in the fifth loading cycle on strain rate for the two strain amplitudes v_1 and v_2. The graph displays the ratio between the peak stresses P_i obtained in the last load cycle for each strain rate r_i, i=1, 2, 3, 4, respectively, and the peak stress P_1 in the slowest cycle with rate r_1

Figure 8 shows the progression of ρ_a and ρ_l at the reversal points of the quasi-static preconditioning protocol (Q) for one representative sample. The difference between the nominal and the in-plane strain is more or less symmetrically distributed around zero and does not exceed 0.0068 (5% of the applied nominal strain). This indicates that the observed deviations are supposedly of a stochastic nature, in addition influenced by the digital image correlation on wet tissue surfaces. Thus, no systematic slippage of the sample could be detected with the current evaluation method, which implies that the clamping worked satisfactorily. Furthermore, ρ_l does not exceed 0.009 (5% of the applied nominal strain).

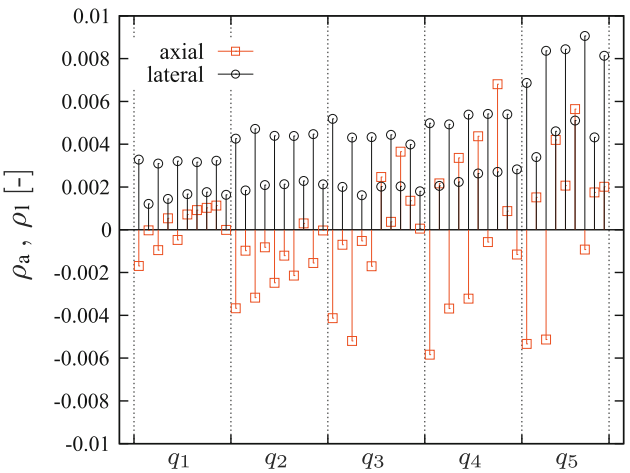

Fig. 8 Difference ρ_a between nominal and measured axial in-plane strains and lateral in-plane strains ρ_l evaluated at the reversal points of the quasi-static preconditioning protocol (Q)

4 Discussion

4.1 Mechanical behaviour of porcine dermis

Like the majority of soft biological tissues, porcine dermis shows transient preconditioning behaviour in cyclic loading experiments. The softening characteristics resemble observations in rubber-like materials (see e.g. Itskov et al. 2006). This concerns in particular the dependence on the strain history known as Mullins effect (Mullins 1947) and the substantial amount of residual strains accumulating during the course of the experiment. Similar behaviour has been reported for murine skin samples excised longitudinally from the abdominal wall (Muñoz et al. 2008). The observed softening may be explained by damage on the one hand and alterations of the microstructure on the other hand. Since softening occurs even at small strains within the range of physiological loading, damage is unlikely in this domain, well possible, however, for higher strains. Microstructural alterations comprise particularly the alignment, reorientation and uncrimping of the collagen network (see e.g. Sellaro et al. 2007). The high content of collagen in the dermal layer might thus as well explain the remarkably large residual strains observed for this type of tissue.

Cyclic loading at varying strain rates reveals viscoelastic properties of the dermal tissue. Soft biological tissues are often reported to be insensitive to strain rate over a wide range (e.g. Fung 1993). Our results suggest that the sensitivity to strain rate depends on the strain amplitude applied during the cyclic loading. Generally, we observed an increase of both, the overall stiffness (Fig. 6) and the peak stress (Fig. 7), with respect to strain rate. The rate dependence was, however, less pronounced for cyclic loading at the higher strain level v_2. Moreover, the slope of the peak stress decreases with strain rate (Fig. 7) and, indeed, the curves may approach a limit at higher rates. Also, the different stabilisation behaviour during the initial cycles at the strain rate of 0.002 s^{-1} (Fig. 6) suggests a dependence of the viscoelastic behaviour on the strain amplitude.

The observed strain and strain rate-dependent viscoelastic properties suggest different mechanisms taking place on the microstructural level. For moderate strains, the interaction of the proteoglycan-rich ground substance with the orienting and uncrimping collagen fibres might dominate the response. For large strains or at high loading rates, where the fibres are not given the time for uncrimping in the viscous gel-like ground substance, the mechanical properties of the collagen fibres itself may become crucial. These assumptions serve to explain the observed behaviour and are supported by recent experimental findings in tendons (Puxkandl et al. 2002).

Comparing the longitudinal and transverse response (Fig. 7), the fibre orientation appears to have a minor effect on the increase in the peak stress ratio indicating that anisotropy is substantially less pronounced in the viscoelastic than in the purely elastic properties.

4.2 Pure shear testing in comparison with uniaxial and biaxial tension

Pure shear testing provides a number of advantages over classic uni- and biaxial testing procedures. Since most soft tissues are subject to biaxial loading in vivo, the pure shear test is much closer to physiological conditions than the uniaxial tension test, while maintaining experimental simplicity. The sample size of 30×60 mm with a final testing aspect ratio of 1:6 turned out to be a good compromise between approximation of the ideal case of pure shear and optimal use of the available sample material. This is confirmed by the optical measurements of the in-plane strains (cf. Sect. 3.3). Although we did not measure stresses in the lateral direction, their presence was indicated by a specimen that failed in a fracture mode, in which the tissue ruptured perpendicular to the axis of loading (Fig. 9).

The test can be performed on a standard uniaxial testing machine by adapting the clamping interfaces to mount pure shear samples. Fixation of the samples itself is easily accomplished by metal grips equipped with sandpaper strips. The wide shape of the pure shear specimens, however, allows for an enlarged contact area between sandpaper and tissue. Accordingly, better fixation is obtained as a result of the increased frictional area, see Sect. 3.3. Moreover, the shorter free lateral boundaries in comparison with uniaxial tension specimens imply a reduced influence of the sample edges, which are particularly prone to be flawed by sample preparation as discussed in Sect. 1.

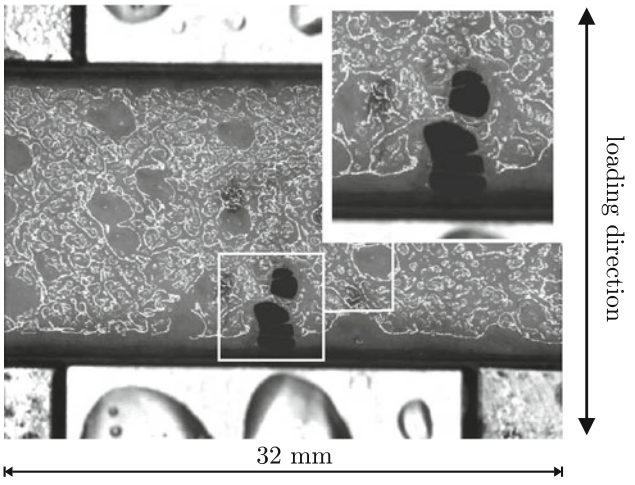

Fig. 9 Failure of a transversal specimen: the tissue ruptured perpendicular to the axis of loading, which indicates the presence of significant stresses in the lateral direction during the pure shear tests

Uniaxial tension specimens are not trivial to handle. For example, their lateral edges tend to roll in due to slight residual stresses in the tissue, and when mounting the samples to the testing device, already gravity deforms the soft specimens. This is not only cumbersome from a technical point of view but also complicates the definition of the initial dimensions of the specimen such as length, width and cross-sectional area, which turns out to be a challenging issue. After mounting the specimen, a slight preload is applied, which is negligible in comparison with the target loads reached in the course of the experiments. The dimensions measured at this preload are taken as reference values for the calculation of the strains. As a result of the low initial stiffness of soft biological tissues and the small cross-sectional area of uniaxial tensile specimens, already these small forces can cause substantial deformations. Moreover, these deformations are to a large extent affected by the above-mentioned cutting artefacts. As a result, the definition of the reference state is somewhat imprecise and not well repeatable, which causes variations in the stress–strain curves of different specimens. Since pure shear specimens of the same thickness provide much more resistance, both, to the unavoidable initial loads and the applied preload, the problems mentioned above are considerably less significant.

From a kinematical point of view, stress or strain controlled biaxial tests provides a useful testing modality which allows for different ratios between tension or extension in two orthogonal in-plane directions. In fact, these tests are standard in many fields of material characterisation such as rubber or metal testing. For soft biological tissues, however, sample preparation, and in particular mounting, poses a fundamental challenge. Either cruciform specimens are rigidly clamped in a testing device with orthogonal loading axes (Waldman and Lee 2005) or square cut samples are flexibly fixed by sutures (Lanir and Fung 1974; Demer and Yin 1983), surgical staples (Sacks 1999), tiny fishing hooks (Boriek et al. 2000) or magnetic tapes (Humphrey et al. 1986). The preparation of cruciform specimens requires a relatively large section of the tissue with preferably homogeneous properties. Moreover, the arms of the cruciform specimens affect the strain field in the central sample area of interest to a large extent so that cases with big strain differences in the two extension directions are difficult to realise. Flexible mounting by sutures or hooks, on the other hand, induces strong local deformations, an inhomogeneous strain field as well as damage at the points where the fixation devices enter the tissue. At higher loads, stress concentration around these points may cause premature failure. In both gripping techniques, inhomogeneity and local anisotropy of the tissue may lead to shearing and rigid rotations of the tissue (see the discussion in Waldman and Lee 2005).

A major advantage of pure shear tests is the highly defined kinematic state obtained. A homogenous state of deformation provided, the only degree of freedom is given by the controllable axial stretch, while the lateral direction is constrained and the thickness change follows from the incompressibility constraint. This clearly simplifies the parameter identification process.

As a critical remark, we would like to emphasise that pure shear tests alone are not sufficient to fully characterise the anisotropic behaviour of soft biological tissues, just as little as other standard tests (see Holzapfel and Ogden 2009, for a discussion of this issue). However, well-defined experimental procedures and accurate data form an essential basis.

In the current study, the tests were not conducted submerged in a saline bath, which would have provided optimal humidification and a controllable temperature. The oscillatory movement of the clamps would have caused wave formation and rendered optical displacement measurement impossible. Nevertheless, the saline solution sprayed onto the specimen accumulated in the narrow gap between the metal grips and formed a closed fluid film on top of the sample so that satisfactory wetting of the tissue was ensured.

4.3 Testing of dermatome-cut tissue samples

Mechanical characterisation of biological tissues in vitro is a controversial issue. On the one hand, excision of the sample from its physiological surroundings changes the mechanical properties, which leads to an immediate relief of residual stresses and creates artificial tissue boundaries. On the other hand, in vitro testing allows for standardised and well-defined experimental conditions. As a necessary requirement, the specimens have to be prepared carefully with accurate geometry. The dermatome allows to create tissue sections of small uniform thickness in the range between 100–1,000 μm, depending on the used dermatome. Moreover, the punching tools guarantee a precise geometry of the specimens in the loading plane. The dermatomes are designed to perform extremely smooth sectioning in plastic and reconstructive surgery and for this reason are predestined for the preparation of evenly shaped specimens without significant damage. Dermatomes and blades exist in different sizes so that the method may be applied to a variety of tissues. The cutting technique is simple, fast and does not require surgical skills.

In particular, in the example of the skin, the proposed method allows for a layer-by-layer characterisation in order to create a detailed three-dimensional mechanical map of the tissue. Beyond that, the thin, fairly translucent specimens are suitable for further histological investigations and microscopical studies. This includes light scattering methods (Ferdman and Yannas 1993) as well as polarisation and confocal laser scanning microscopy (Meyer et al. 1982; Vardaxis et al. 1997).

5 Conclusions

We presented a robust and highly defined testing method for soft biological tissues. The key features include the use of a surgical dermatome and pure shear testing. The results suggest that the ideal pure shear state was adequately achieved by simple and inexpensive means with a standard materials testing machine available in most laboratories. As a novel method for sample preparation, a surgical dermatome was used in combination with punching dies. This allowed to excise specimens of very accurate thickness and geometry. In the present work, this preparation procedure was applied to porcine skin, but it is applicable to a variety of other soft tissues. The precise geometry of the samples and the accurate control over initial and boundary conditions (cf. Sect. 4.2) in pure shear indicate a general reduction in the systematic errors in comparison with classic uniaxial and biaxial testing. This will have to be proven statistically on a broader database in the future. This concerns both, the defined slicing procedure as well as the pure shear testing. A first set of pure shear data on porcine dermis is presented herein and is available for interpretation. The observed behaviour is to a large extent consistent with typical characteristics of soft tissues. A more detailed analysis of the results incorporating modelling of the dermis by means of an adequate constitutive formulation will follow and be provided elsewhere.

Acknowledgments We are grateful to Prof. Dr. med. A. Prescher, University Hospital Aachen, for advising us of the use of a dermatome in order to cut thin skin sections. We thank Dr. med. M. Guggenheim, University Hospital Zurich, for providing the dermatome, explaining its use and for his kind support concerning questions on anatomy and histology of the skin. Partial funding was provided by the Swiss National Science Foundation (NCCR CO-ME). The authors would also like to gratefully acknowledge both anonymous reviewers for many helpful critical comments on the first version of this paper.

References

Bonifasi-Lista C, Lake SP, Small MS, Weiss JA (2005) Viscoelastic properties of the human medial collateral ligament under longitudinal, transverse and shear loading. J Orthop Res 23(1):67–76

Boriek AM, Kelly NG, Rodarte JR, Wilson TA (2000) Biaxial constitutive relations for the passive canine diaphragm. J Appl Physiol 89(6):2187–2190

Brouwer I, Ustin J, Bentley LS, A Dhruv N, Tendick F (2001) Measuring in vivo animal soft tissue properties for haptic modeling in surgical simulation. Stud Health Technol Inform 81:69–74

Butler DL, Grood ES, Noyes FR, Zernicke RF, Brackett K (1984) Effects of structure and strain measurement technique on the material properties of young human tendons and fascia. J Biomech 17(8):579–596

Carter FJ, Frank TG, Davies PJ, McLean D, Cuschieri A (2001) Measurements and modelling of the compliance of human and porcine organs. Med Image Anal 5(4):231–236

Chu BM, Fraher WG, Wayland H (1972) Hysteretic behavior of soft living animal tissue. Ann Biomed Eng 1(2):182–203

Cox HT (1942) The clevage lines of the skin. Br J Surg 29(144):234–240

Delalleau A, Josse G, Lagarde J, Zahouani H, Bergheau J (2006) Characterization of the mechanical properties of skin by inverse analysis combined with the indentation test. J Biomech 39(9):1603–1610

Demer LL, Yin FCP (1983) Passive biaxial mechanical properties of isolated canine myocardium. J Physiol 339:615–630

Dobrev HP (1999) In vivo study of skin mechanical properties in patients with systemic sclerosis. J Am Acad Dermatol 40(3):436–442

Dokos S, Smaill B, Young A, LeGrice I (2002) Shear properties of passive ventricular myocardium. Am J Physiol Heart Circ Physiol 283(6):H2650–H2659

Ferdman A, Yannas I (1993) Scattering of light from histologic sections: a new method for the analysis of connective tissue. J Invest Dermatol 100(5):710–716

Fung YC (1993) Biomechanics: mechanical properties of living tissues: 2nd edn. Springer, New York

Gao Z, Lister K, Desai J (2009) Constitutive modeling of liver tissue: experiment and theory. Ann Biomed Eng 83(2):502–516

Holzapfel GA, Ogden RW (2009) On planar biaxial tests for anisotropic nonlinearly elastic solids. A continuum mechanical framework. Mathe Mech Solids 14:474–489

Holzapfel GA, Sommer G, Gasser CT, Regitnig P (2005) Determination of layer-specific mechanical properties of human coronary arteries with nonatherosclerotic intimal thickening and related constitutive modeling. Am J Physiol Heart Circ Physiol 289(5):H2048–H2058

Humphrey JD, Vawter DL, Vito RP (1986) Mechanical-behavior of excised canine visceral pleura. Ann Biomed Eng 14(5):451–466

Itskov M, Haberstroh E, Ehret A, Voehringer M (2006) Experimental observation of the deformation induced anisotropy of the Mullins effectin rubber. KGK Kautschuk Gummi Kunststoffe 3(3):93–96

Kalanovic D, Ottensmeyer M, Gross J, Buess G, Dawson S (2003) Independent testing of soft tissue visco-elasticity using indentation and rotary shear deformations. Stud Health Technol Inform 94:137–143

Klatt D, Hamhaber U, Asbach P, Braun J, Sack I (2007) Noninvasive assessment of the rheological behavior of human organs using multifrequency mr elastography: a study of brain and liver viscoelasticity. Phys Med Biol 52(24):7281–7294

Korhonen RK, Laasanen MS, Töyräs J, Rieppo J, Hirvonen J, Helminen HJ, Jurvelin JS (2002) Comparison of the equilibrium response of articular cartilage in unconfined compression, confined compression and indentation. J Biomech 35(7):903–909

Langer K (1861) Zur Anatomie und Physiologie der Haut. I. Über die Spaltbarkeit der Cutis In: British Journal of Plastic Surgery 31, 3–8 (1978). Sitzungsbericht der Mathematisch-naturwissenschaftlichen Classe der Kaiserlichen Academie der Wissenschaften 44(1):19–46

Lanir Y, Fung YC (1974) Two-dimensional mechanical properties of rabbit skin-II. Experimental results. J Biomech 7(2):171–182

Mathews MB (1975) Connective tissue, molecular biology, biochemistry and biophysics. Springer, Berlin

Meyer W, Neurand K, Radke B (1981) Elastic fibre arrangement in the skin of the pig. Arch Dermatol Res 270(4):391–401

Meyer W, Neurand K, Radke B (1982) Collagen fibre arrangement in the skin of the pig. J Anat 139(148):134

Miller K (2005) Method of testing very soft biological tissues in compression. J Biomech 38(1):153–158

Mullins L (1947) Effect of stretching on the properties of rubber. J Rubber Res 16:275–289

Muñoz M, Bea J, Rodríguez J, Ochoa I, Grasa J, Pérez del Palomar A, Zaragoza P, Osta R, Doblaré M (2008) An experimental study of the mouse skin behaviour: damage and inelastic aspects. J Biomech 41(1):93–99

Nava A, Mazza E, Furrer M, Villiger P, Reinhart W (2008) In vivo mechanical characterization of human liver. Med Image Anal 12(2):203–216

Ottensmeyer M (2002) Tempest I-D: an instrument for measuring solid organ soft tissue properties. Exp Tech 26(3):48–50

Puxkandl R, Zizak I, Paris O, Keckes J, Tesch W, Bernstorff S, Purslow P, Fratzl P (2002) Viscoelastic properties of collagen: synchrotron radiation investigations and structural model. Philos Trans R Soc B 357(1418):191–197

Ridge MD, Wright V (1966) The directional effects of skin. A bio-engineering study of skin with particular reference to Langer's lines. J Invest Dermatol 46(4):341–346

Rouvière O, Yin M, Dresner M, Rossman P, Burgart L, Fidler J, Ehman R (2006) MR elastography of the liver: preliminary results. Radiology 240(2):440–448

Sacks MS (1999) A method for planar biaxial mechanical testing that includes in-plane shear. J Biomech Eng 121(5):551–555

Sacks MS (2000) Biaxial mechanical evaluation of planar biological materials. J Elast 61(1–3):199–246

Sandrin L, Fourquet B, Hasquenoph J, Yon S, Fournier C, Mal F, Christidis C, Ziol M, Poulet B, Kazemi F, Beaugrand M, Palau R (2003) Transient elastography: a new noninvasive method for assessment of hepatic fibrosis. Ultrasound Med Biol 29(12): 1705–1713

Sellaro TL, Hildebrand D, Lu Q, Vyavahare N, Scott M, Sacks MS (2007) Effects of collagen fiber orientation on the response of biologically derived soft tissue biomaterials to cyclic loading. J Biomed Mater Res 80(1):197–205

Valtorta D, Mazza E (2006) Measurement of rheological properties of soft biological tissue with a novel torsional resonator device. Rheol Acta 45(5):677–692

Van Loocke M, Lyons C, Simms C (2008) Viscoelastic properties of passive skeletal muscle in compression: stress-relaxation behaviour and constitutive modelling. J Biomech 41(7):1555–1566

Vardaxis N, Brans T, Boon M, Kreis R, Marres L (1997) Confocal laser scanning microscopy of porcine skin: implications for human wound healing studies. J Anat 190:601–611

Waldman SD, Lee JM (2005) Effect of sample geometry on the apparent biaxial mechanical behaviour of planar connective tissues. Biomaterials 26(35):7504–7513

Wineman A, Wilson D, Melvin JW (1979) Material identification of soft-tissue using membrane inflation. J Biomech 12(11):841–850

Zernicke RF, Butler DL, Grood ES, Hefzy MS (1984) Strain topography of human tendon and fascia. J Biomech Eng 106(2):177–180